1999

Modulation of the Bursting Properties of Single Mouse Pancreatic β-Cells by Artificial Conductances

T.A. Kinard
Virginia Commonwealth University

G. de Vries
University of Alberta

A. Sherman
National Institutes of Health

L. S. Satin
Virginia Commonwealth University, lsatin@hsc.vcu.edu

Modulation of the Bursting Properties of Single Mouse Pancreatic β-Cells by Artificial Conductances

T. A. Kinard,* G. de Vries,# A. Sherman,§ and L. S. Satin*

*Departments of Pharmacology and Toxicology and Physiology, Medical College of Virginia, Virginia Commonwealth University, Richmond, Viginia 23298-0524 USA; #Department of Mathematical Sciences, University of Alberta, Edmonton, Alberta T6G 2G1, Canada; and §Mathematical Research Branch, National Institute of Diabetes, Digestive and Kidney Diseases, National Institutes of Health, Bethesda, Maryland 20892 USA

ABSTRACT Glucose triggers bursting activity in pancreatic islets, which mediates the Ca^{2+} uptake that triggers insulin secretion. Aside from the channel mechanism responsible for bursting, which remains unsettled, it is not clear whether bursting is an endogenous property of individual β-cells or requires an electrically coupled islet. While many workers report stochastic firing or quasibursting in single cells, a few reports describe single-cell bursts much longer (minutes) than those of islets (15–60 s). We studied the behavior of single cells systematically to help resolve this issue. Perforated patch recordings were made from single mouse β-cells or hamster insulinoma tumor cells in current clamp at 30–35°C, using standard K^+-rich pipette solution and external solutions containing 11.1 mM glucose. Dynamic clamp was used to apply artificial K_{ATP} and Ca^{2+} channel conductances to cells in current clamp to assess the role of Ca^{2+} and K_{ATP} channels in single cell firing. The electrical activity we observed in mouse β-cells was heterogeneous, with three basic patterns encountered: 1) repetitive fast spiking; 2) fast spikes superimposed on brief (<5 s) plateaus; or 3) periodic plateaus of longer duration (10–20 s) with small spikes. Pattern 2 was most similar to islet bursting but was significantly faster. Burst plateaus lasting on the order of minutes were only observed when recordings were made from cell clusters. Adding g_{Ca} to cells increased the depolarizing drive of bursting and lengthened the plateaus, whereas adding g_{KATP} hyperpolarized the cells and lengthened the silent phases. Adding g_{Ca} and g_{KATP} together did not cancel out their individual effects but could induce robust bursts that resembled those of islets, and with increased period. These added currents had no slow components, indicating that the mechanisms of physiological bursting are likely to be endogenous to single β-cells. It is unlikely that the fast bursting (class 2) was due to oscillations in g_{KATP} because it persisted in 100 μM tolbutamide. The ability of small exogenous currents to modify β-cell firing patterns supports the hypothesis that single cells contain the necessary mechanisms for bursting but often fail to exhibit this behavior because of heterogeneity of cell parameters.

INTRODUCTION

When exposed to stimulatory levels of glucose (>7 mM), pancreatic islets of Langerhans secrete insulin (reviewed in Ashcroft and Rorsman, 1989b; Satin and Smolen, 1994). A component of this stimulus-secretion coupling pathway is the appearance of bursting electrical activity in the islet after the suppression of islet K_{ATP} channels (reviewed in Ashcroft and Rorsman, 1989a; Satin, 1996). When recorded with sharp microelectrodes, islet bursting in 11.1 mM glucose consists of rhythmic slow plateau waves that depolarize islets from −65 to about −40 mV for 10 s (Dean and Matthews, 1968, 1970a,b; Atwater et al., 1978; Henquin, 1987; Ribalet and Beigelman, 1980; Cook, 1984). Riding on these slow plateaus are rapid, Ca^{2+}-dependent voltage spikes ~40 ms in duration, which further depolarize the islet to ~ −10 mV (Fig. 1). During the silent interburst period, pacemaker potentials depolarize the islet to the threshold of the next plateau. This pattern of electrical activity likely involves complex interactions between many different β-cell ion channels, although the detailed ionic mechanism of this phenomenon remains unresolved (reviewed in Cook et al., 1991; Satin and Smolen, 1994; Sherman, 1996). The Ca^{2+} uptake associated with Ca^{2+} channel activity during the depolarizing spikes and plateaus is a major contributor to the rise in intracellular free $[Ca^{2+}]$, which stimulates insulin exocytosis. In support of this view, it has been shown that pulsatile insulin release occurs roughly in phase with the burst plateaus (Rosario et al., 1986; Henquin, 1987).

Attempts to understand the ionic basis of islet bursting have come mainly from studies of the ion channel currents of cultured rat, mouse, or insulinoma β-cells or membrane patches from these cells (Ashcroft and Rorsman, 1989a,b; Satin and Smolen, 1994; Cook et al., 1991). However, classic bursting is observed in intact mouse islets. Since islets are a syncytium of up to 3000 or so electrically-coupled cells (Bonner-Weir et al., 1989), it has been suggested that maintaining this electrically coupled network is mandatory for physiological bursting (Sherman, 1996). Thus it has been proposed that only whole islets or large clusters of electrically coupled cells burst, whereas single cells cannot, because coupling is needed to defeat either cell-cell heterogeneity (Smolen et al., 1993; Misler et al., 1991) or the disruptive effect of stochastic channel gating

Received for publication 11 March 1998 and in final form 16 November 1998.

Address reprint requests to Dr. L. S. Satin, Department of Pharmacology and Toxicology, Medical College of Virginia Campus, Virginia Commonwealth University, Box 980524, Richmond, VA 23298-0524. Tel.: 804-828-7823; Fax: 804-828-1532; E-mail: lsatin@hsc.vcu.edu.

0006-3495/99/03/1423/13 $2.00

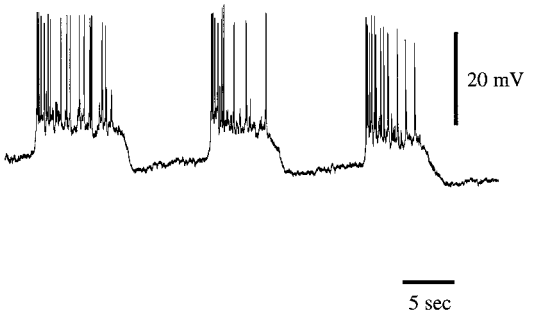

FIGURE 1 Bursting activity in an intact mouse islet exposed to 11.1 mM glucose and recorded with sharp microelectrodes. Note the drop-off in spike frequency during individual bursts, and the pacemaker potential during interbursts, followed by the rapid upstroke of the plateau wave. Many bursts show spike-free plateaus just before repolarization to the silent phase.

when the total pool of channels is relatively small (Atwater et al., 1981; Sherman et al., 1988).

These hypotheses, of course, are not mutually exclusive. However, one difficulty in assessing the importance of cell-cell coupling for bursting is that much less is known about the electrical behavior of single, isolated β-cells than what is known about intact islets. Specifically, it is not clear how reliably single cells burst. Thus, whereas Smith et al. (1990) and Larsson et al. (1996) observed slow (e.g., 1 min long), glucose-dependent bursting in single mouse β-cells or small clusters of cells, other investigators observed stochastic spiking or quasibursting in single rodent β-cells (e.g., Misler et al., 1992) rather than robust bursting.

To understand single islet cell firing and its contribution to whole islet bursting, we used perforated patch clamp to systematically reexamine the firing characteristics of single, completely isolated mouse islet cells at 35°C. We first wished to determine whether β-cells burst endogenously in 11.1 mM glucose, as do whole islets. We then used a novel electrophysiological technique called dynamic clamping (Sharp et al., 1993; O'Neil et al., 1995; Satin et al., 1996) to determine how titrating varying amounts of artificial g_{KATP} and g_{Ca} affected these electrical properties.

We report here that the electrical activity of single mouse β-cells is heterogeneous and includes both bursting and nonbursting patterns. Bursting could be observed both endogenously and after some small intervention on our part. This bursting was generally fast compared to the usual burst pattern of intact islets, but it could also be induced to resemble islet bursting. Exceedingly small changes in artificial K_{ATP} conductances applied with dynamic clamp had a large impact on the membrane potential and firing behavior of single cells when they were near their firing threshold. Activation of K_{ATP} channels after metabolic inhibition hyperpolarized single mouse β-cells, and dynamic clamping could be used to subtract artificial g_{KATP}, allowing us to estimate the endogenous whole-cell g_{KATP}. Adding g_{KATP} with g_{Ca} potentiated electrical activity, producing activity which resembled that of whole islets. These results suggest that single mouse β-cells exist in a regime where bursting occurs endogenously or are close to it, so that a small perturbation can move them into that regime. In addition, because the fast bursting in single cells persisted when K_{ATP} channels were blocked with tolbutamide, it is unlikely that the cyclic activation of K_{ATP} channels is involved in this burst pattern.

MATERIALS AND METHODS

Cell culture

Mouse pancreases were isolated from Swiss-Webster mice by collagenase digestion to yield single islets, as previously described (Hopkins et al., 1991; Kinard and Satin, 1996). Islets were dispersed into single cells by gently shaking them in a low-calcium medium. Mouse β-cells were cultured in RPMI-1640 medium supplemented with fetal bovine serum, L-glutamine, and penicillin/streptomycin. Over 80% of islet cells cultured with this approach can be shown by immunocytohistochemistry to be β-cells (Hopkins et al., 1991). β-Cells can also be identified by their diameter (10–12 μm). Insulin-secreting hamster insulinoma tumor (HIT) cells HIT-T15 were cultured in Ham's F-12 medium and passaged weekly with trypsin-EDTA as previously described (Santerre et al., 1981; Satin and Cook, 1988; Satin et al., 1994). HIT cells used were from passages 50–70. Mouse β-cells and HIT cells were seeded onto glass coverslips in 35-mm Petri plates and kept at 37°C in an air/CO_2 incubator and were fed every 2–3 days. To avoid electrical artifacts due to cell-cell coupling, only isolated single cells were selected for study, except where noted. Only mouse β-cells were used for studies of single-cell bursting, because in our hands, HIT cells exhibit only repetitive spiking rather than bursting.

Electrophysiology and solutions

Mouse β-cells or HIT cells were placed in a recording chamber affixed to the stage of an inverted microscope (Olympus IM-T2 or IX50). The chamber was continuously superfused with an external solution that contained (in mM) 115 NaCl, 3 $CaCl_2$, 5 KCl, 2 $MgCl_2$, 10 HEPES, 11.1 glucose (pH 7.2). Because HIT cells are more sensitive to glucose (Satin et al., 1995; Santerre et al., 1981), the external solution used to study HIT cells contained 1 mM glucose and 120 mM NaCl. In perforated patch experiments (Falke et al., 1989) pipette tips were filled with a solution that contained (in mM) 28.4 K_2SO_4, 63.7 KCl, 11.8 NaCl, 1 $MgCl_2$, 20.8 HEPES, 0.5 EGTA (pH 7.2). The pipettes were then back-filled with the same internal solution containing 0.1 mg/ml amphotericin B. The electrode was then placed on a cell, and gigaohmic seals were obtained. It usually took 5–15 min to obtain adequate steady-state patch perforation, and experiments did not commence until a steady zero current potential was obtained.

Solutions containing tolbutamide or sodium azide were made fresh daily. The HIT cell experiments were carried out at room temperature (20–22°C), and mouse β-cells experiments were performed at 35°C. The recording chamber was heated with a TC-1 temperature controller and an H-1 heater (Cell Micro Controls, Virginia Beach, VA). The bath temperature was measured at the bottom surface of the recording chamber with a TH-1 thermocouple probe. An Axopatch-1D patch-clamp amplifier (Axon Instruments, Foster City, CA) was used in the standard tight-seal perforated patch-clamp mode to analyze membrane potential under current-clamp conditions (Hamill et al., 1981). Seal resistances obtained ranged from 5 to 20 GΩ.

Dynamic clamping

Dynamic clamping was used to titrate different amounts of artificial conductance into single cells to determine the effects of these conductances on cell membrane potential and electrical activity (Sharp et al., 1993; Ma

and Koester, 1996; Turrigiano et al., 1996; Satin et al., 1996). This is achieved by injecting current but differs from the standard current clamp technique in that the amount injected is based on the calculated response of a hypothetical voltage-dependent current to the membrane potential of the cell at each instant. This has the effect of changing the time course of the potential, including the apparent input resistance of the cell, as if a channel with the given activation and inactivation properties and reversal potential were activated in the cell membrane. Dynamic clamp differs from both current clamp and voltage clamp, including physiological waveform clamp (Satin et al., 1994), in that the intervention is determined by dynamic feedback rather than being set in advance. The approach is a hybrid between pure experimentation and pure modeling, as it requires a model with assumed properties for only one or a few ionic currents, rather than a complete model of the cell. Within the limitations described below, the response of the intact cell machinery to the modeled current can be explored.

To implement dynamic clamp, membrane potential (V_m) was rapidly sampled via a 12-bit A/D-D/A board (Digidata 1200; Axon Instruments) in current clamp and scaled appropriately. Artificial currents based on the measured V_m were calculated in software (Dclamp; Dyna-Quest Technologies, Sudbury, MA) and scaled appropriately, and a driving voltage was sent out through the D/A converter to inject the artificial currents into a patch-clamped cell in real time. The membrane potential was then rapidly resampled and the process continued. The clock speed of the computer determines the speed with which the Dclamp program updates membrane potential (O'Neil et al., 1995). Therefore we used a fast computer (Pentium 133 MHz; Micron Electronics, Nampa, ID) and acquisition system to make it possible to sample membrane potentials at >10 kHz. The parameters determining the injected currents in the model equation were set by the experimenter during individual experiments. However, the software used here required temporary deactivation of the dynamic clamp while these parameters were changed.

Artificial K_{ATP} current was calculated as

$$I_{KATP} = g_{KATP}(V_K - V_m), \quad (1)$$

where g_{KATP} was varied on-line and V_K was set at −90 mV. Although Eq. 1 makes the assumption that I_{KATP} is linear whereas physiological I_{KATP} shows weak inward rectification (Ashcroft and Rorsman, 1995), endogenous K_{ATP} current is reasonably linear over the physiological voltage range (Rorsman and Trube, 1985; Cook and Hales, 1984). Artificial I_{KATP} current thus corresponds to the quasiphysiological current that would be expected to flow if the conductance set by this theoretical equation became activated in the cell. A limitation of this approach in the case of I_{KATP} is that dynamic clamp can only mimic the electrical manifestations of g_{KATP} activation but not the modulation of endogenous I_{KATP} by intracellular nucleotides or other factors. This limitation is not critical for I_{KATP}, but difficulty in tracking $[Ca^{2+}]_i$ on a fast enough time scale prevents introduction of artificial Ca^{2+}-activated K^+ current into cells.

Artificial voltage-gated Ca^{2+} current was calculated according to the Hodgkin-Huxley formalism,

$$I_{Ca} = g_{Ca}mh(V_{Ca} - V_m), \quad (2)$$

where the maximum conductance g_{Ca} was varied on-line and V_{Ca} was set at +100 mV. The activation (m) and inactivation (h) variables were calculated by

$$\frac{dm}{dt} = \alpha_m(1 - m) - \beta_m m, \quad (3)$$

$$\frac{dh}{dt} = \alpha_h(1 - h) - \beta_h h, \quad (4)$$

$$\alpha_m, \beta_m, \alpha_h, \beta_h = \frac{a}{1 + \exp((d + Vm)/f)}, \quad (5)$$

The free parameters a, d, and f are listed in Table 1 *A*; they were selected to produce an artificial Ca^{2+} current resembling native β-cell Ca^{2+} current (e.g., Rorsman and Trube, 1986; Sherman et al., 1988), but lacking the slow inactivation process described by Satin and Cook (1989). These equations and parameters yielded a current-voltage (*I-V*) relationship for Ca^{2+} current that started activating at −60 mV, peaked at −10 mV, and became asymptotic as the voltage approached +100 mV, the theoretical reversal potential for I_{Ca}. The time constant for activation, $1/(\alpha_m + \beta_m)$, was 0.1 ms, and the time constant for inactivation, $1/(\alpha_h + \beta_h)$, was 1 ms. Note that the artifical Ca^{2+} current intentionally lacked slow inactivation (described by Satin and Cook, 1988, 1989; Cook et al., 1991). It also did not directly gate the influx of Ca^{2+} ions into the cells. However, despite these simplifications, injection of artificial g_{Ca} strongly modified the firing of single cells, in some cases producing oscillatory electrical activity.

TABLE 1 Values of the free parameters used in Eq. 5

	a (s)	d (mV)	f (mV)
A			
α_m	10,000	−4	−14
β_m	10,000	−4	14
α_h	1,000	10	10
β_h	1,000	10	−10
B			
α_m	0.1	−4	−14
β_m	0.1	−4	14
α_h	0.04	10	10
β_h	0.04	10	−10

A: Values used for the artificial Ca^{2+} current injected into single mouse β-cells via dynamic clamp. Activation and inactivation kinetics are fast. B: Values used for the artificial Ca^{2+} current imposed on a passive RC circuit for validation of the dynamic clamp setup. Activation and inactivation kinetics are slow.

Validation of dynamic clamp using a passive RC circuit

To verify the dynamic clamp method, an artificial K_{ATP} conductance, calculated according to Eq. 1, was applied to a passive single section RC circuit consisting of a 10-GΩ resistor in parallel with a 5-pF capacitor. Table 2 shows that the measured and theoretical voltage responses obtained using different values for g_{KATP} were quite comparable.

Next we applied an artificial slow, voltage-gated Ca^{2+} conductance, described by standard Hodgkin-Huxley equations (Eqs. 2–5), to the RC circuit. The parameters chosen (Table 1 *B*) equipped the channel with slow activation and inactivation kinetics. This was done to facilitate bench testing and analysis of the dynamic clamp system. Fig. 2 demonstrates that a theoretical simulation of this experiment (*dotted lines*) closely (within 5–10%) predicted the membrane potentials observed with the passive model. Upon activation of dynamic clamp, membrane potential depolarized from 0 mV (the initial condition) to a maximum that progressively increased as g_{Ca} increased. Peak depolarization was recorded within 10 s after a depolarization phase, and the membrane potentials then slowly repolarized toward a new steady state. Limitations of the dynamic clamp technique were most apparent for conductances below 0.02 nS, which

TABLE 2 Measured and theoretical responses to different levels of g_{KATP} imposed on a passive RC circuit

g_{KATP} (nS)	Measured V_m (mV)	Theoretical V_m (mV)
0.01	−8.0	−8.1
0.1	−48	−45
1.0	−89	−81.8

Theoretical responses were calculated as $V_m = g_{KATP}V_K/(g_{KATP} + 0.1)$.

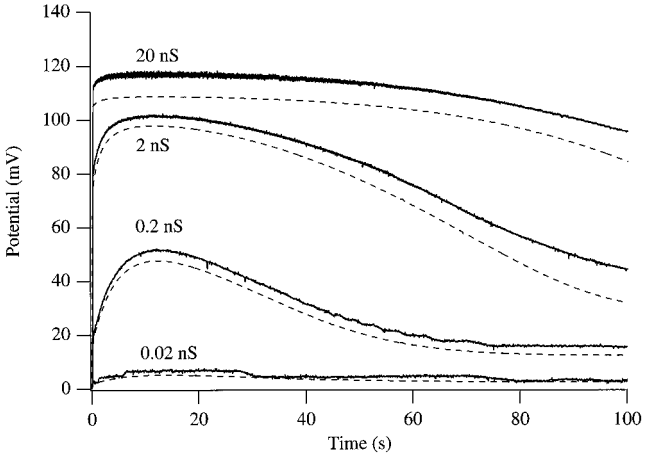

FIGURE 2 Verification of the dynamic clamp method. Solid lines represent the voltage responses to imposed levels of g_{KATP} (0.02, 0.2, 2.0, or 20 nS) using a passive RC circuit. The dotted lines represent the voltages expected from Eqs. 2–5 and the parameter values from Table 1 *B*.

approach the 12-bit resolution of our D/A board, or conductances greater than 10 nS. We thus limited our studies to the 0.1–2.0-nS conductance range for g_{KATP} and g_{Ca}.

Data analysis

Driving voltages sent out from the D/A board were filtered at 10 kHz, and cell membrane potentials were acquired at 20 kHz with a PCM-based VCR recorder (DR 8900; Neurodata Corp.) for off-line analysis. For playback, taped voltage data were digitized at 200 Hz after low-pass filtering at 100 Hz. Data acquisition and analysis were carried out with a Macintosh Quadra 800 computer (Apple Computer, Cupertino, CA), a 16-bit, 200-kHz hardware interface (Instrutech, Elmont, NY), IgorPro 3.0 software (Wavemetrics, Lake Oswego, OR), and Pulse Control software (Herrington and Bookman, 1994).

To present the varied cell firing behaviors in a condensed form, cells were classified by visual inspection into three broad categories, plateau cells, bursters, and spikers, based on characteristics such as spike amplitude, period, and the existence of plateau depolarizations (Fig. 3). We further calculated three summary statistics, each a single number that characterizes a representative 60-s sample of firing activity. One is the "activity fraction," the fraction of time the cell spent above a threshold level. For cells with plateaus, the traces were first smoothed by spline interpolation to remove spikes and small fluctuations, so that the activity fraction for those cells is equivalent to the plateau fraction commonly used in studies of bursting islets. Cells with only spiking activity were smoothed minimally. The threshold crossings also yielded an average cycle (spike or plateau) period. As values can be sensitive to choice of threshold, a second measure of activity was obtained by constructing a histogram of all of the data points in a trace (Fig. 4). Each histogram was fit to a sum of two Gaussians, of the form

$$G(V_m) = L_a \exp[-((V_m - L_c)/L_w)^2] + R_a \exp[-((V_m - R_c)/R_w)^2]$$

with amplitudes L_a and R_a, centers L_c and R_c, and widths L_w and R_w. The activity fraction was then estimated by the "delta peak," the normalized difference in peak amplitudes of the Gaussians:

$$\Delta_p = 100(L_a - R_a)/\max(L_a, R_a)$$

The delta peak scores, Δ_p, lie between −100 and +100. The two measures of activity obtained by thresholding and from the peak differential are not independent because the thresholds were obtained from the Gaussian fit. However, plotting the two measures against each other visually separates the classes of bursters and displays the trends in the data better than either one alone (see Fig. 5 *A*). The overlap between the classes is partly reflective of the difficulty in distinguishing the different behaviors unambiguously, especially between bursters and spikers.

Firing patterns described in the paper were representative of recordings from at least 52 single islet cells. Results obtained in the dynamic clamp experiments were representative of at least four cells. Some aspects of these investigations have appeared in abstract form (Kinard et al., 1997).

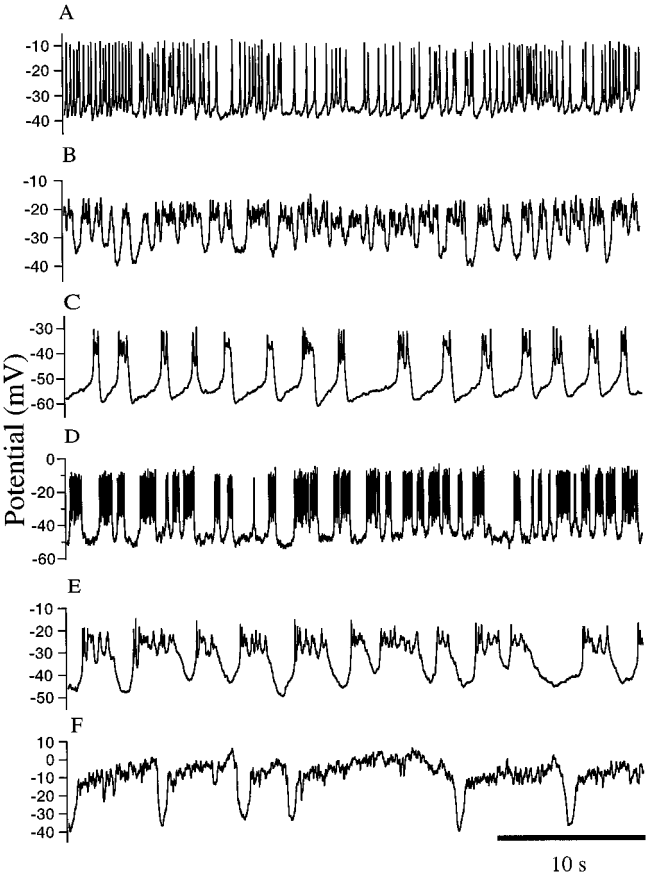

FIGURE 3 Representative patterns of electrical activity recorded in single mouse β-cells. (*A*) Example of a class I cell, showing repetitive fast spikes. (*B–E*) Examples of class II cells, showing fast spikes superimposed upon relatively brief periodic depolarizations. The cell in *C* exhibits a pacemaker potential, as observed in bursting activity in intact islets (Fig. 1). Silent phases ranged from −60 to −40 mV; the plateau phase was from −35 to −10 mV. The transition from the silent phase to the plateau phase was abrupt in all cases. (*F*) Example of a class III cell, showing periodic plateaus of longer duration without clear spikes.

RESULTS

The electrical properties of single cultured mouse β-cells

Single mouse β-cells and HIT cells exhibited rapid spiking in suprathreshold glucose. Most cells began to exhibit electrical activity at a threshold voltage ranging from −55 to −40 mV. In some cases it was necessary to inject small (~5 pA) currents to polarize cells to voltages where sustained

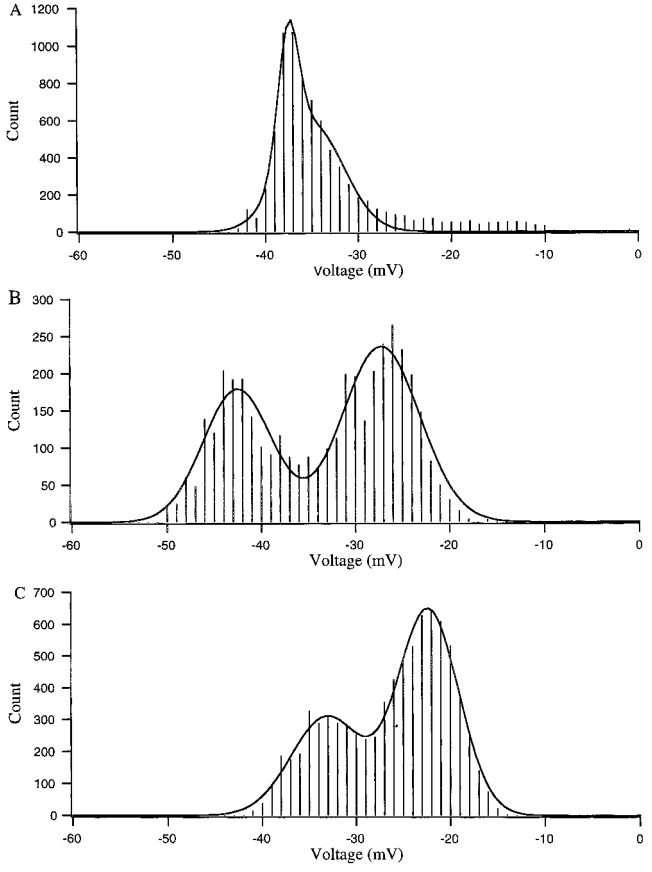

FIGURE 4 Amplitude histograms representing the three classes (1, 2, 3) of bursting. Each histogram was fit to a sum of two Gaussians (see text). (*A*) Histogram from a cell that was spiking (see Fig. 3 *A*). (*B*) A representative histogram from a bursting cell (Fig. 3 *B*). (*C*) Taken from a plateau cell (Fig. 3 *F*).

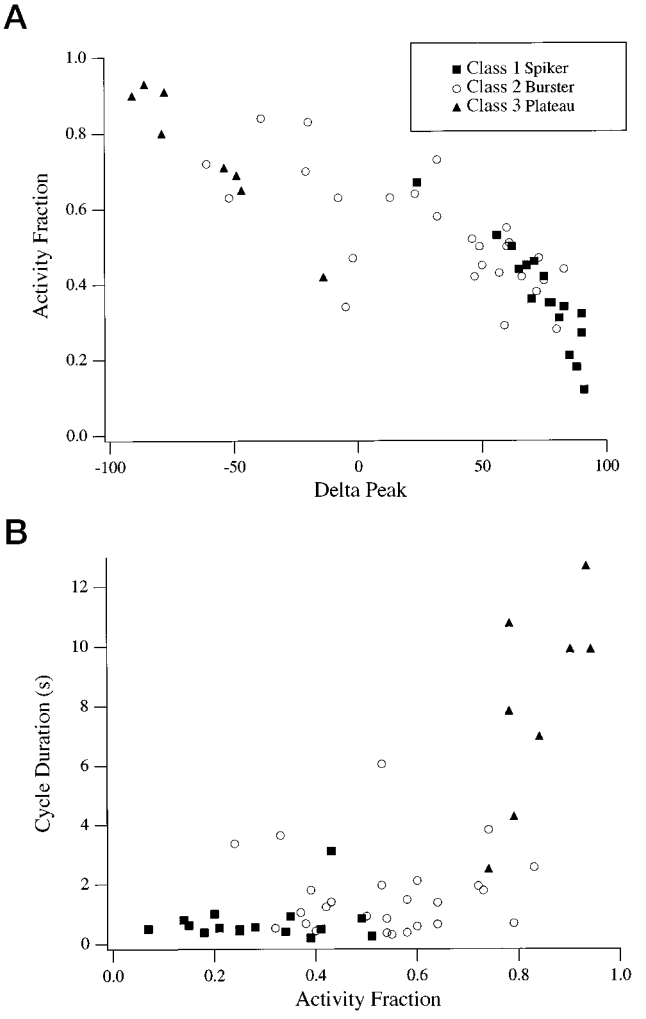

FIGURE 5 Summary statistics of heterogeneous firing patterns. (*A*) The activity fraction determined by thresholding was plotted against the delta peak from amplitude histograms (Fig. 4; see text) and cycle duration. (*B*) Cycle durations from thresholding were plotted versus activity fraction.

and robust bursting occurred. Only mouse β-cells showed clear clustering of spikes into bursts, although the firing properties of single mouse β-cells were in general quite heterogeneous (Misler et al., 1991). HIT cells only showed repetitive spiking and did not burst. Mouse β-cells, in contrast, could be grouped (see Materials and Methods) into three basic categories: 1) cells with repetitive, generally larger fast spikes ($n = 17$; 33% of the population studied); 2) cells with small-amplitude fast spikes superimposed upon relatively brief (<5 s) plateau depolarizations ($n = 27$; 52%); or 3) cells with periodic plateaus of longer duration (10–20 s) with small fluctuations riding upon them ($n = 8$; 15%).

Burst pattern 2 most closely resembled islet bursting but was significantly faster. We will refer to the former as "fast bursting" and the latter as "regular bursting." Representative samples of the electrical activity of single mouse β-cells are shown in Fig. 3. These cells showed spiking, bursting, and plateau activity at voltages ranging from ~−60 to 0 mV. Fig. 3 *A* shows a class 1 spiking cell; Fig. 3, *B–E*, shows examples of class 2 cells; and Fig. 3 *F* is a class 3 cell.

Unlike the electrical behavior of whole islets (Fig. 1), it was often difficult to clearly distinguish spikes from plateau depolarizations in isolated cells (e.g., Fig. 3, *B*, *E*, and *F*). In addition, the pacemaker depolarizations, which are clearly evident during the interburst periods in islets (Fig. 1), were only evident in some single cells (e.g., Fig. 3 *C*). It was generally the case that whereas spike clustering could be conspicuous in single cells, the durations of the burst, plateau, or interburst periods were far more irregular than in whole islets. In a few cases, cells exhibited regularly occurring plateau events with few clear spike events (Fig. 3 *F*). It was also generally the case that recordings from single cells exhibited far more voltage noise than is seen in whole islets (compare recordings in Fig. 3 versus those in Fig. 1), possibly because of increased channel noise (Atwater et al., 1978; Sherman et al., 1988).

Fig. 5 *A* shows the two measures of cell activity level (see Materials and Methods), activity fraction and Δ_p, plotted against each other for all of the cells in the data set. The

class 1 cells generally had the smallest values of activity fraction and the largest values of Δ_p, corresponding to histograms with a large left peak and small right peak (Fig. 4 *A*). Note that although these cells spiked continuously, their activity fractions are low because the spikes spend most of their time at more negative membrane potentials. This is the opposite of what one would see with continuously spiking cells in islets exposed to high (~20 mM) glucose; these would have large activity fractions and depolarized average membrane potentials. Class 3 cells had histograms with a larger right peak (Fig. 4 *C*) and were typified by large activity fraction and small Δ_p. The class 2 cells had the most diverse patterns (Fig. 3, *B–E*) and, correspondingly, the broadest range of scores in both activity parameters.

The cycle durations were shortest on average for class 1 (0.72 ± 0.17 s; (mean ± SEM), longest for class 3 (8.1 ± 1.2 s), and intermediate for class 2 (1.6 ± 0.27 s). No apparent correlation was obtained between cycle duration and activity fraction or Δ_p within classes 1 and 2 (Fig. 5 *B*). Within Class 2 cycle duration correlated positively with activity fraction (0.71) and negatively with Δ_p (−0.67).

Our observations encompass the range of bursting or spiking behavior previously described in the literature from studies of single cells, with one notable exception. Unlike results reported by Smith et al. (1990) and Larsson et al. (1996), we did not observe "ultraslow bursting," that is, bursting with plateau depolarizations lasting on the order of minutes in single mouse β-cells. However, we could on occasion observe long plateaus of this type when recording from obvious cell clusters (Kinard and Satin, unpublished observations). This activity may thus be more characteristic of small clusters of β-cells rather than single cells; when selecting cells for patching, it can often be difficult to distinguish the two.

The effects of imposed g_{KATP} on single-cell electrical activity

Very small changes in artificial K_{ATP} conductances applied with dynamic clamp could have a large impact on the membrane potential and firing behavior of mouse β- and HIT cells. The mouse β-cell shown in Fig. 6, for example, was initially firing fast bursts from ~ −30 mV. Adding 0.15 nS of g_{KATP} (*horizontal bar*) rapidly hyperpolarized this cell from −30 to −55 mV and largely inhibited firing such that only a few action potentials were observed after increased g_{KATP}. Terminating the dynamic clamp rapidly restored fast firing. Assuming the single-channel conductance of K_{ATP} in physiological saline to be 15 pS (Fatherazi and Cook, 1991), 0.15 nS of g_{KATP} represents the opening, on average, of 10 extra K_{ATP} channels. Applying 0.14 nS of g_{KATP}, representing the opening of only one less K_{ATP} channel, produced strikingly less inhibition of firing and resulted in an intermediate bursting pattern (Fig. 6 *c*). Upon removal of the dynamic clamp, the cell again returned to its original firing pattern.

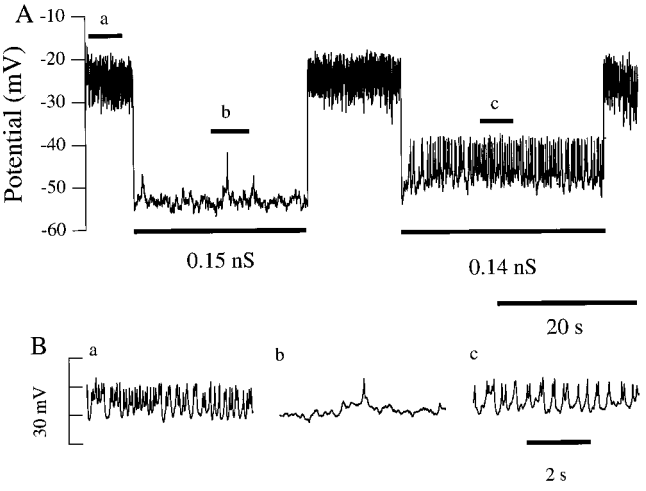

FIGURE 6 Titration of g_{KATP} into a single mouse β-cell, using dynamic clamp. (*A*) Exceedingly small currents could strongly modulate firing activity in single mouse β-cells. Horizontal bars indicate periods when dynamic clamp was applied. (*B*) Sections from Fig. 4 *A*, indicated by *a*, *b*, and *c*, shown on an expanded time scale.

It was also possible to significantly modulate HIT cell firing by using small quantities of g_{KATP}. Fig. 7 shows a representative HIT cell that was initially firing spikes from ~ −45 mV. HIT cells spikes were typically large (≥30 mV) and brief relative to mouse spikes. We did not see bursting in HIT cells (but see Keahy et al., 1989). Adding 0.1 nS of g_{KATP} hyperpolarized this cell to near −55 mV and significantly decreased its spike frequency. This effect reversed upon removal of g_{KATP}. The transient acceleration of spike frequency seen here after moderate sojourns to hyperpolarized potentials was observed in both HIT and mouse β-cells.

Thus small K_{ATP} conductances were able to significantly alter the membrane potential and electrical activity of mouse β-cells and HIT cells. This strongly suggests that both types of insulin-secreting cells are exquisitely attuned to the opening and closing of small numbers of K_{ATP} channels. This was particularly true near the firing threshold of the cells, because even the closing of one additional K_{ATP} channel moved the cell from rest to repetitive firing.

Fig. 8, *A* and *B*, shows that the titration of increasing amounts of g_{KATP} into a single mouse β-cell progressively suppressed its electrical activity and hyperpolarized its membrane potential, as shown earlier. In this cell, the addition of 0.03–0.06 nS of g_{KATP} was associated with irregular burstlike spiking. The spiking threshold of the cell occurred at ~0.06 nS, whereas levels of g_{KATP} greater than 0.06 nS produced longer hyperpolarizations that completely inhibited firing.

Upon termination of dynamic clamp after prolonged (>10 s) and deep hyperpolarizations associated with 0.5–1.0 nS of g_{KATP}, we observed a slow depolarization phase that lacked spikes and lasted more than 5 s before the cell returned to a rapid firing mode (Fig. 8, *Ae* and *Be*). This is in contrast to the increased spike frequency usually ob-

served after more moderate hyperpolarizations (e.g., Fig. 7). Interestingly, hyperpolarizations produced by the application of somatostatin or galanin lead to similar slow, spike-free depolarization when these hormones are removed (Abel et al., 1996; Ashcroft and Rorsman, 1995).

Fig. 9 summarizes results obtained using dynamic clamp to add g_{KATP} to single mouse β-cells and HIT cells. Application of 0–1.0 nS of artificial g_{KATP} progressively hyperpolarized cell membrane potentials up to −40 mV and decreased electrical activity. The responses of HIT cells and mouse cells were similar, as shown. This range of g_{KATP} mimics the effect of adding 3–67 open K_{ATP} channels to the cell membrane. The maximum sensitivity of membrane potential to added g_{KATP} occurred with 0.1–0.3 nS of g_{KATP}. Because the amplitude of these V_m deflections reflects the divergence of V_m from V_K, the tight distribution obtained reflects the fairly tight distribution of the control membrane potentials.

Dynamic clamping and DC current injection had similar but not identical effects on β-cell electrical activity

The single mouse β-cell shown in Fig. 10 was clearly bursting when DC current was applied to hold the cell near −55 mV (the *black bar* denotes the period of current injection). When this current was switched off, the cell abruptly depolarized by ~10 mV and began firing ~10 mV plateau-like events of a fast nature. However, these quickly subsided (Fig. 10 *B* is a continuation of Fig. 10 *A*). The cell then was hyperpolarized to −60 mV, after the injection of 0.5 nS of g_{KATP} via dynamic clamp. Immediately after the hyperpolarization we observed a slow (1–3 s) depolarizing "creep" or rebound, which triggered increased firing (see also Fig. 12 *Ab*, *c*, *e*). We have also observed creep with DC current injection (data not shown), so it is not an artifact of the dynamic clamp. After the creep, the cell showed burst-like events, similar to the bursts seen with injected current, but with smaller spikes during the bursts. When the dynamic clamp was switched off, the cell again abruptly depolarized and began firing rapid plateau-like events as before. Restoration of DC current injection to repolarize the cell to −55 mV again (Fig. 10 *C*) restored the original fast activity shown in Fig. 10 *A*.

One does not expect injection of DC current and injection of a membrane conductance to have identical effects on electrical activity, because the latter decreases input resistance (i.e., acts as a shunt). Indeed, this may explain why the spikes observed when dynamic clamp conductance was added were smaller than those seen with simple current injection.

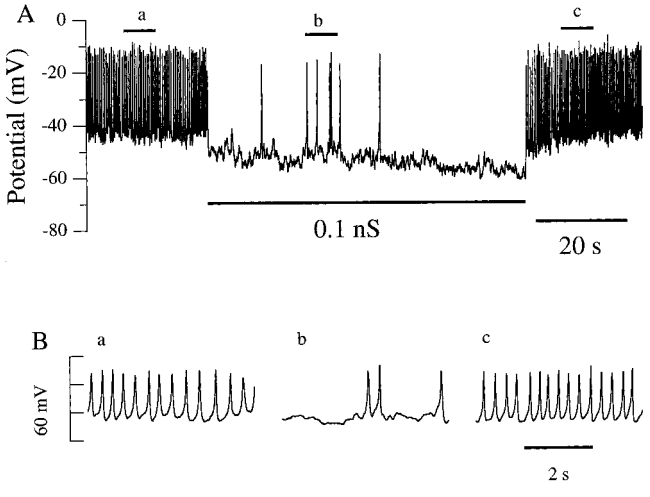

FIGURE 7 Titration of g_{KATP} into a single HIT cell. (*A*) Addition of 0.1 nS of g_{KATP} with dynamic clamp reversibly hyperpolarized the cell and decreased cell firing. (*B*) Sections from Fig. 5 *A*, shown on an expanded time scale.

Poisoning β-cells to maximally activate K_{ATP} channels yields an estimate of whole-cell g_{KATP}

To estimate the maximum K_{ATP} conductance of the mouse β-cell and compare it to the artificial g_{KATP} values injected, we applied the metabolic inhibitor sodium azide to inhibit metabolism (Misler et al., 1986; Larsson et al., 1996). The fall in the ATP/ADP ratio due to azide would be expected to maximally activate K_{ATP} channels, resulting in β-cell hyperpolarization (Cook and Hales, 1984; Ashcroft et al., 1984; Misler et al., 1986). After cell hyperpolarization, dynamic clamp was then used to "subtract" rather than add artificial g_{KATP} to null out the hyperpolarization and return the cell to its original firing pattern. The value of artificial g_{KATP} subtracted should approximate the amount of endogenous g_{KATP} activated after cell poisoning.

Fig. 11 shows that the application of 5 mM sodium azide hyperpolarized mouse β-cells as expected, in this case by 28 mV, taking membrane potential from −38 to −66 mV. The subsequent subtraction of 0.1 nS of g_{KATP} depolarized the cell by ~10 mV, whereas subtracting 1 nS of g_{KATP} nearly reversed the poisoning-induced hyperpolarization. This is the converse of the observations of Henquin (1992), who found that addition of the K_{ATP} channel opener diazoxide was not equivalent to the removal of glucose. The mean amplitude of azide-induced hyperpolarization in six cells was −21.8 ± 5.6 mV (mean ± SEM). Restoration of near-control values of V_m was attained by subtracting 1.09 ± 1.13 nS ($n = 6$) of artificial g_{KATP} (range 0.2–3 nS). This suggests that single mouse β-cells have a maximum g_{KATP} that ranges from 0.2 to 3 nS. Calculations based on determinations of K_{ATP} density in membrane patches have yielded estimates of g_{KATP} ranging from 0.27 to 7.6 nS (Ashcroft et al., 1984; Misler et al., 1986), whereas Cook et al. (1988) estimated that β-cells had as much as 15 nS g_{KATP}. Whole-cell patch-clamp measurements of Rorsman and Trube (1986), made using cells dialyzed with ATP-free pipette solutions, yielded a total g_{KATP} of 3–10 nS.

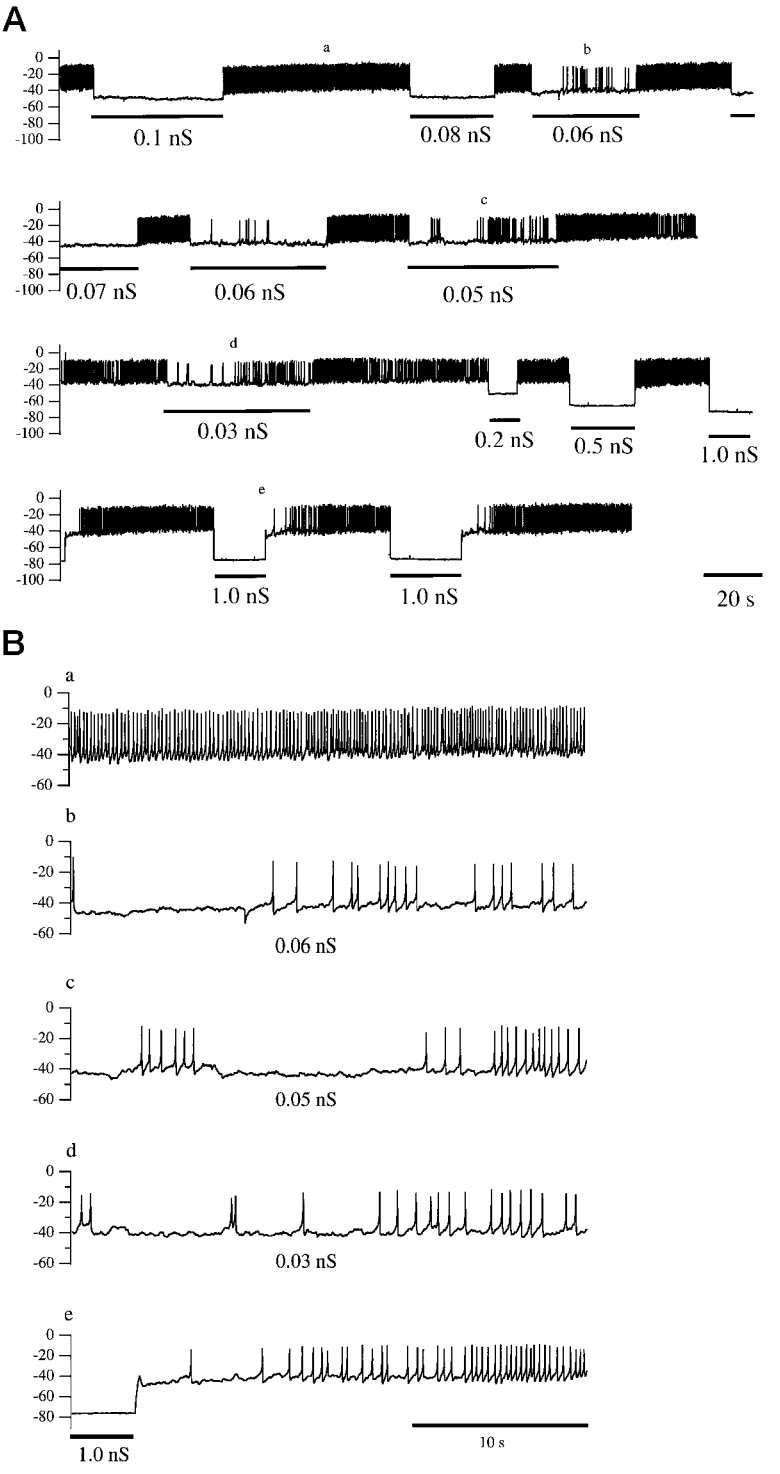

FIGURE 8 Titration of varying amounts of g_{KATP} into a single mouse β-cell. (*A*) Increasing amounts of g_{KATP} progressively hyperpolarized cell membrane potential. (*B*) Sections *A* shown on an expanded time scale. After the deep hyperpolarization in *e*, the cell exhibited a slow depolarization phase that lacked spikes and lasted more than 5 s before the rapid firing mode was restored.

The addition of artificial g_{KATP} and g_{Ca} to single bursting mouse β-cells potentiated bursting and increased its regularity

Removing Ca_o blocks bursting in intact islets (Ribalet and Beigelman, 1981; Meissner and Schmeer, 1981) and isolated β-cells (Kinard et al., 1998). Although it is known that islet bursting is dependent on $[Ca^{2+}]$, it is not clear how Ca^{2+} channel activity quantitatively contributes to islet bursting. To test the relative importance of Ca^{2+} conductance for bursting in single β-cells, we used dynamic clamp to inject an artificial Ca^{2+} conductance in addition to artificial K_{ATP} conductance. The properties of the artificial voltage-gated Ca^{2+} current are described in Materials and Methods.

In the absence of dynamic clamp conductances, the mouse β-cell shown in Fig. 12 was initially exhibiting an irregular fast bursting pattern. The application of increasing

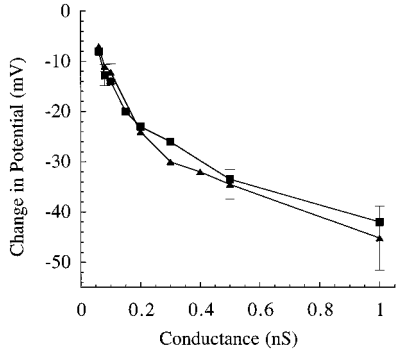

FIGURE 9 Summary of changes in V_m (mean ± SEM) produced in HIT (▲, n = 1–8) and mouse β-cells (■, n = 1–3) after the addition of varying amounts of g_{KATP} with dynamic clamp. The mean change in V_m increased with increasing g_{KATP} (0.06–1.0 nS) from −7 to −45 mV in HIT and from −8 to −42 mV in mouse β-cells.

amounts of g_{KATP} (0.05, 0.08, or 0.1 nS) to the cell progressively hyperpolarized the β-cell membrane potential and inhibited cell firing, as was found earlier. Injected currents were also able to modulate the firing pattern as described previously.

Whereas the application of 0.1 nS or more of artificial K_{ATP} currents hyperpolarized the cell and inhibited cell firing, the simultaneous application of a modest amount of artificial Ca^{2+} current led to the reappearance of activity, albeit of an irregular nature (compare Fig. 12, *Ab* and *Ac*). Note that the coapplication of g_{KATP} and g_{Ca} did not tend to cancel their individual effects (n = 7). Rather, increasing g_{Ca} increased the depolarizing drive and resulted in more

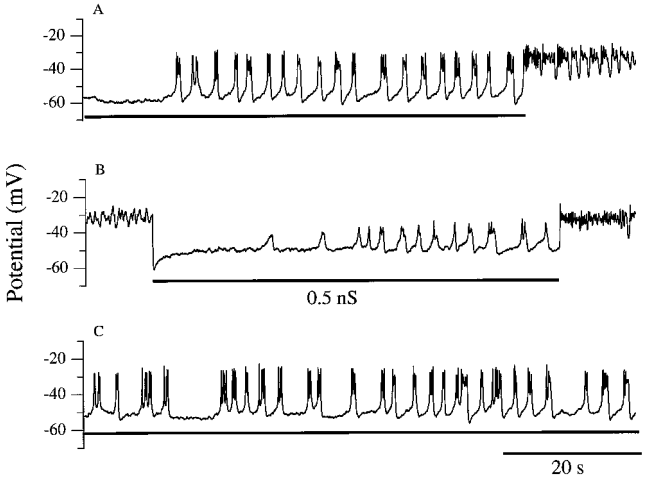

FIGURE 10 Comparison of the effect of injection of DC current and injection of dynamic clamp conductances on a single mouse β-cell. (*A*) During injection of 1.8 ± 0.9 pA of DC current, the cell exhibited clear bursting activity, with deep silent phases. Upon removal of the current, the cell depolarized and reverted to fast, irregular firing activity. (*B*) After injection of 0.5 nS g_{KATP}, the cell exhibited a slow depolarizing creep before exhibiting clear bursting. Note that the bursts observed during dynamic clamping are smaller than those seen with DC current injection. (*C*) Injection of the same DC current as in *A* restored the bursting activity seen in *A*.

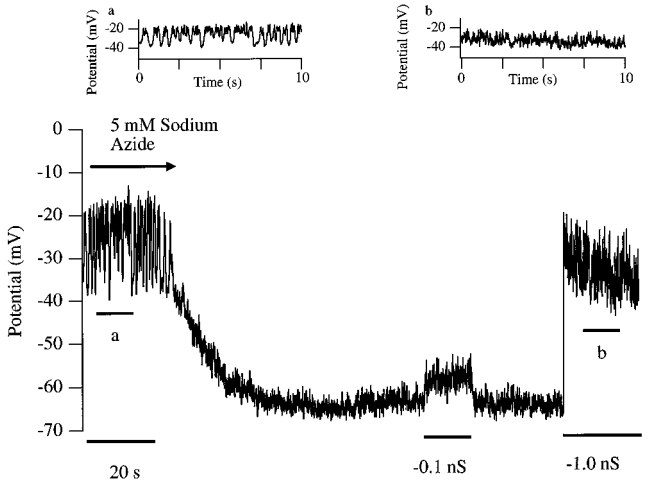

FIGURE 11 Quantitation of g_{KATP} by poisoning. The addition of 5 mM sodium azide hyperpolarized single mouse β-cells within 2 min. Dynamic clamping was then used to subtract artificial g_{KATP} to restore original firing pattern. In this cell, the subtraction of 1 nS of g_{KATP} counterbalanced the effect of azide on membrane potential, suggesting that ~1 nS of endogenous g_{KATP} was originally activated by metabolic inhibition.

pronounced burst activity (compare Fig. 12 *Ac* with *Ad*, and *Fig.* 12 *Ae* with *Af*), whereas adding g_{KATP} increased the hyperpolarizing drive and (compare Fig. 12 *Af* with *Ag*) and resulted in more pronounced silent phases. Adding just the right balance of g_{KATP} and g_{Ca} led to a slower burst pattern, resembling the electrical activity observed in intact mouse islets (Fig. 1; Kitasato et al., 1996; Ribalet and Beigelman, 1980), as shown in Fig. 12 *Ag*. Application of different amounts of these currents failed to induce the islet-like burst pattern in general, thus indicating the need for a delicate balance of K_{ATP} and Ca^{2+} conductances.

The islet-like bursting was observed despite the fact that neither the artificial K_{ATP} nor Ca^{2+} conductances were equipped with slow variables, i.e., they lacked any intrinsic slow rhythmicity. This suggests that the mechanism for producing islet-like bursting is endogenous to single β-cells; our experimental manipulations modified the cell state in such a way that the endogenous slow oscillatory mechanism could be expressed.

A closer examination of the islet-like burst pattern (Fig. 12 *Bg*) shows aspects of both the original fast burst pattern of the cell (Fig. 12 *Ba*) and the much slower oscillation brought out by our experimental manipulations. During each plateau episode in the slow burst pattern, small and brief hyperpolarizations can be seen, similar to the ones characterizing the original fast burst pattern. This suggests a competition between two different endogenous burst mechanisms, where each may operate on its own time scale.

Altering g_{Ca} relative to g_{KATP} produced a variety of electrical activity in a single β-cells, ranging from fast bursting with small spikes to large and more prolonged periodic plateaus completely lacking spikes. Although we cannot account for the plateau versus fast spiking or fast bursting patterns we have observed in single cells (Fig. 3),

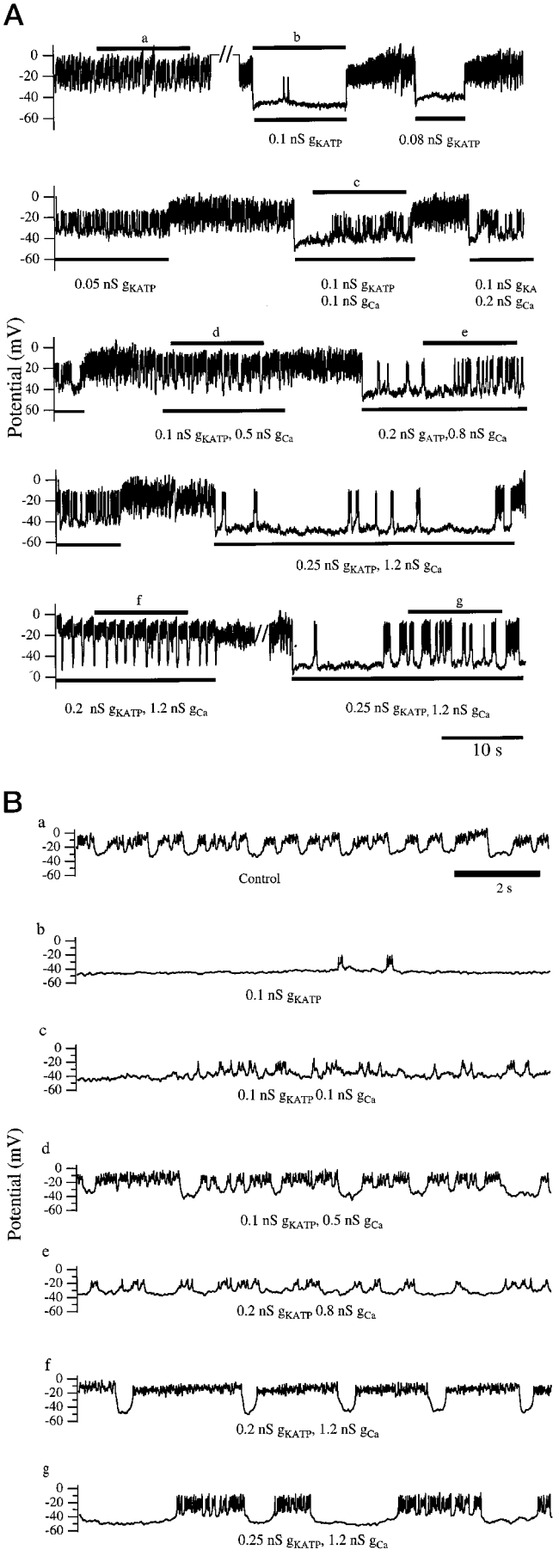

FIGURE 12 Effect of titrating g_{KATP} and g_{Ca} on the electrical activity of a single mouse β-cell. (*A*) Injection of g_{KATP} alone has a hyperpolarizing effect. Injection of g_{Ca} in addition to g_{KATP} improves bursting activity and may induce islet-like bursting. See text for details. (*B*) Sections from 10 *A* shown on an expanded time scale.

subtle alterations in the amount of g_{Ca} relative to g_{KATP} were sufficient to switch among these behaviors. This suggests that the diversity of patterns is due to quantitatively small variations in cell properties, possibly including but not limited to channel densities, rather than qualitative differences.

Effects of tolbutamide on the electrical activity of single β-cells

Because there is likely to be some residual g_{KATP} left in 11.1 mM glucose (Cook and Ikeuchi, 1989; Ashcroft and Rorsman, 1989a), we tested the effect of adding 100 μM tolbutamide on single β-cell electrical activity. It has been reported that tolbutamide at this dose fully blocks endogenous g_{KATP} (Trube et al., 1986; Sturgess et al., 1985). In our hands, the addition 100 μM of tolbutamide to single mouse β-cells had a modest but consistent effect, producing a depolarization of 4.8 $\pm$ 0.8 mV (n = 5). Significantly, tolbutamide did not abolish the fast bursting pattern associated with single β-cells.

For example, Fig. 13 shows a single mouse β-cell bathed in 11.1 mM glucose, which displayed a clear bursting pattern. The addition of 100 μM tolbutamide modestly depolarized the cell interburst potential but clearly did not abolish or even significantly modulate the bursting pattern. This suggests that K_{ATP} channels are unlikely to be mediating the fast single cell electrical bursting. Restoration of near-control membrane potentials, using dynamic clamp to reverse the action of tolbutamide, also had little or no effect on fast bursting (data not shown). We cannot rule out, however, that the ultraslow bursting in single cells reported by others and the regular bursting observed in islets are mediated by slow changes in g_{KATP}, perhaps because of oscillations in cell metabolism.

DISCUSSION

Single mouse β-cells are heterogeneous and can burst

We have now recorded the electrical activity from many single mouse β-cells. Although a large number of these cells exhibited rapid firing, we also routinely observed cells with clearly established bursting activity, even without any intervention (injection of DC current or dynamic clamp) on our part. Typically, the bursting activity observed was an order of magnitude faster than islet bursting. However, occasionally, single cell bursts on the time scale of an islet were also observed.

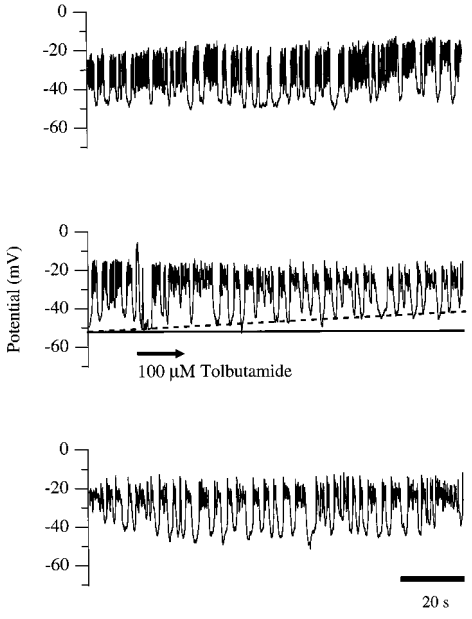

FIGURE 13 The addition of 100 μM tolbutamide to a bursting mouse β-cell produced modest depolarization but did not eliminate bursting.

Before this study it was not clear from the literature whether bursting was a general characteristic of single β-cells. Two brief reports (Smith et al., 1990; Larsson et al., 1996) described a type of bursting in single β-cells characterized by unusually long plateaus (several minutes long) compared to the plateaus observed in islets (5–10 s long). Most reports have suggested that single β-cells show either stochastic spiking activity or quasibursting.

We also found that small perturbations of the cell, such as the injection of small DC currents or the application of artificial conductances, can have large modulatory effects. In Fig. 10, for example, a small amount of hyperpolarizing DC current converted fast bursts to somewhat slower bursts with much larger amplitudes. Of particular note are the effects of simultaneously adding modest amounts of g_{KATP} and g_{Ca} via dynamic clamp, as shown in Fig. 12. Injecting g_{Ca} in addition to g_{KATP} increased the robustness of bursting and the burst amplitude, while decreasing burst frequency. In some cells, the addition of both artificial conductances induced a very robust form of bursting, similar to that of intact mouse islets. Neither the artificial K_{ATP} current nor the artificial Ca^{2+} current was equipped with any slow time constants in these experiments.

These results are consistent with the "heterogeneity hypothesis" of Smolen et al. (1993), who proposed that the mechanisms for bursting are endogenous to each cell, but that bursting may not be realized in some single cells because parameters lie outside the narrow bursting regime. Our experimental manipulations introduce additional perturbations to the cell, which can return the cell to its bursting regime. Heterogeneity may persist even in islets but may be difficult to observe because the cells are well synchronized by electrical coupling.

The induced islet-like burst pattern shown in of Fig. 12 *Bg* occurred on a slower time scale than the cell's original fast burst pattern. However, during the plateau phase of the induced burst, the small and brief hyperpolarizing events that characterized the original fast burst pattern were still observed. This suggests that there may be at least two burst mechanisms endogenous to single β-cells.

Fast bursting in single cells does not appear to require oscillations in g_{KATP}

To test the hypothesis that oscillations of the ATP/ADP ratio mediate the bursts, as was proposed for islets (Larsson et al., 1996; Dryselius et al., 1994), we examined the electrical activity of single mouse β-cells under conditions where the endogenous g_{KATP} of the cell was either minimized by a high glucose concentration or eliminated by the application of tolbutamide. In both conditions, we observed fast bursting activity (see Fig. 13). Thus this form of bursting does not appear to require oscillations in g_{KATP} in single mouse β-cells.

Although the fast bursting activity of single cells persisted despite blockade of endogenous K_{ATP} channels by tolbutamide, we cannot rule out the possibility that the ultraslow bursting seen by some other workers is mediated by slow metabolic oscillations that drive changes in g_{KATP}. In addition to demonstrating variation in g_{KATP} between spiking and silent phases, Larsson et al. (1996) reported that tolbutamide converted slow oscillations in cytosolic Ca^{2+} to a steady plateau (but see also recent data from Miura et al. (1997), who sometimes found slow oscillations persisting in saturating doses of tolbutamide). However, we fail to observe this form of bursting in our single mouse β-cells.

Although it appears that g_{KATP} does not play a pacemaker role, at least not for fast bursting, our data confirm that it does play a modulatory role in shaping the firing pattern of the cell. In particular, it plays an important role in setting the firing threshold (Figs. 6 and 7), burst amplitude (Figs. 8, 10, and 12), and interburst interval (Fig. 12).

Slow processes revealed by dynamic clamp

Our experimental manipulations have revealed two processes that occur on time scales much slower than the time scale of the spike activity. The first is a delay in the return to firing upon termination of the dynamic clamp, after a prolonged period of deep hyperpolarization (Fig. 8 *A*, *bottom*). This delay lasts on the order of 5 s. The second slow process is a depolarizing creep in the membrane potential during less extreme hyperpolarizations (Figs. 10 *B* and 12 *Ab*, *c*, *e*). It is conceivable that the creep reflects an underlying slow process that contributes to the pacemaker potential of the interburst period in β-cells and islets because it compensates for hyperpolarization by slowly depolarizing. The ionic basis and functional role of both of these slow processes in bursting remain to be elucidated.

In summary, single mouse β-cell electrical activity was found to be heterogeneous but included burst like behavior and at least two manifestations of underlying slow processes. Single-cell bursting was fast compared to the ultra-slow bursting previously reported to occur in single cells as well as the bursting seen in intact islets. The majority of single cells, whether initially bursting or not, were very sensitive to small changes in channel activity, as revealed by additional dynamic clamp conductances, and could be induced to burst. The range of electrical activity observed when g_{Ca} and g_{KATP} were simultaneously altered suggests that these channels are important determinants of bursting and may contribute to the heterogeneous electrical patterns we observed. Results obtained with the dynamic clamp also show that whatever the identity of the bursting pacemaker channel ultimately turns out to be, exceedingly small currents or conductances may suffice to pace bursting. Last, our data support the hypotheses that islet cells may be electrically coupled within islets to defeat a considerable degree of cell-cell heterogeneity.

All experiments were carried out by TAK and LSS. GdV and AS contributed to the design of experiments and analysis in light of theoretical models. We thank Doug McIntosh for excellent technical assistance and Dan Cook for supplying us with the data shown in Fig. 1.

Work in the laboratory of LSS is supported by the National Institutes of Health (DK46409).

REFERENCES

Abel, K.-B., S. Lehr, and S. Ullrich. 1996. Adrenaline-, not somatostatin-induced hyperpolarization is accompanied by a sustained inhibition of insulin secretion in INS-1 cells. Activation of sulphonylurea K^+_{ATP} channels is not involved. *Pflügers Arch.* 432:89–96.

Ashcroft, F. M., D. E. Harrison, and S. J. H. Ashcroft. 1984. Glucose induces closure of single potassium channels in isolated rat pancreatic β-cells. *Nature.* 312:446–448.

Ashcroft, F. M., and P. Rorsman. 1989a. ATP-sensitive K^+ channels: a link between B-cell metabolism and insulin secretion. *Biochem. Trans.* 18:109–111.

Ashcroft, F. M., and P. Rorsman. 1989b. Electrophysiology of the pancreatic β-cell. *Prog. Biophys. Mol. Biol.* 54:87–143.

Ashcroft, F. M., and P. Rorsman. 1995. Electrophysiology of pancreatic islet cells. *In* The Electrophysiology of Neuroendocrine Cells. H. Scherübl and J. Hescheler. CRC Press, Boca Raton, FL. 207–244.

Atwater, I., C. H. Dawson, G. T. Eddlestone, and E. Rojas. 1981. Voltage noise measurements across the pancreatic β-cell membrane: calcium channel characteristics. *J. Physiol. (Lond.).* 314:195–212.

Atwater, I., B. Ribalet, and E. Rojas. 1978. Cyclic changes in potential and resistance of the B-cell membrane induced by glucose in islets of Langerhans from mouse. *J. Physiol. (Lond.).* 278:117–139.

Bonner-Weir, S., D. Deery, J. L. Leahy, and G. C. Weir. 1989. Compensatory growth of pancreatic beta-cells in adult rats after short-term glucose infusion. *Diabetes.* 38:49–53.

Cook, D. L. 1984. Electrical pacemaker mechanisms of pancreatic islet cells. *FASEB J.* 43:2368–2372.

Cook, D. L., and C. N. Hales. 1984. Intracellular ATP directly blocks K^+ channels in pancreatic B-cells. *Nature.* 311:271–273.

Cook, D. L., and M. Ikeuchi. 1989. Tolbutamide as mimic of glucose on β-cell electrical activity. *Diabetes.* 38:416–421.

Cook, D. L., L. S. Satin, M. L. Ashford, and C. N. Hales. 1988. ATP-sensitive K^+ channels in pancreatic beta-cells. Spare-channel hypothesis. *Diabetes.* 37:495–498.

Cook, D. L., L. S. Satin, and W. F. Hopkins. 1991. Pancreatic B cells are bursting, but how? *Trends Neurosci.* 14:411–414.

Dean, P. M., and E. K. Matthews. 1968. Electrical activity in pancreatic islet cells. *Nature.* 45:389–390.

Dean, P. M., and E. K. Matthews. 1970a. Glucose-induced electrical activity in pancreatic islet cells. *J. Physiol. (Lond.).* 210:255–264.

Dean, P. M., and E. K. Matthews. 1970b. Electrical activity in pancreatic islet cells: effects on ions. *J. Physiol. (Lond.).* 210:265–275.

Dryselius S., P. E. Lund, E. Gylfe, and B. Hellman. 1994. Variations in ATP-sensitive K^+ channel activity provide evidence for inherent metabolic oscillations in pancreatic beta-cells. *Biochem. Biophys. Res. Commun.* 205:880–885.

Falke, L. C., K. D. Gillis, D. M. Pressel, and S. Misler. 1989. "Perforated patch recording" allows long-term monitoring of metabolite-induced electrical activity and voltage-dependent Ca^{2+} currents in pancreatic B cells. *FEBS Lett.* 251:167–172.

Fatherazi, S., and D. L. Cook. 1991. Specificity of tetraethylammonium and quinine for three K channels in insulin-secreting cells. *J. Membr. Biol.* 120:105–144.

Hamill, O. P., A. Marty, E. Neher, B. Sakmann, and F. J. Sigworth. 1981. Improved patch clamp techniques for high-resolution current recordings from cells and cell-free membrane patches. *Pflügers Arch.* 391:85–100.

Henquin, J. C. 1987. Regulation of insulin release by ionic and electrical events in β-cells. *Hormone Res.* 27:168–178.

Henquin, J. C. 1992. Adenosine triphosphate-sensitive K^+ channels may not be the sole regulators of glucose-induced electrical activity in pancreatic β-cells. *Endocrinology.* 131:127–131.

Herrington, J., and R. J. Bookman. 1994. Pulse Control v4.3: Igor XOPs for Patch Clamp Data Acquisition. University of Miami Press, Miami, FL.

Hopkins, W. F., L. S. Satin, and D. L. Cook. 1991. Inactivation kinetics and pharmacology distinguish two calcium currents in mouse pancreatic B-cells. *J. Membr. Biol.* 119:229–239.

Keahy, H., A. Rajan, A. Boyd, III, and D. Kunze. 1989. Characterization of voltage-dependent Ca channels in a beta cell line. *Diabetes.* 38: 188–193.

Kinard, T. A., and L. S. Satin. 1996. Temperature modulates the Ca^{2+} current of HIT-T15 and mouse pancreatic β-cells. *Cell Calcium.* 20: 475–482.

Kinard, T. A., L. S. Satin, G. de Vries, and A. Sherman. 1997. Titrating K_{ATP} conductances into single insulin-secreting cells via dynamic clamp. *Biophys J.* 72:A250.

Kinard, T. A., L. S. Satin, G. de Vries, and A. Sherman. 1998. Single β-cells from mouse pancreatic islets exhibit a fast form of bursting which does not require free [Ca] accumulation. *Biophys. J.* 74:A101.

Kitasato, H., R. Kai, W.-G. Ding, and M. Omatsu-Kanbe. 1996. The intrinsic rhythmicity of spike-burst in pancreatic β-cells and intercellular interaction within an islet. *Jpn. J. Physiol.* 46:363–373.

Larsson, O., H. Kindmark, R. Bränström, B. Fredholm, and P.-O. Berggren. 1996. Oscillations in K_{ATP} channel activity promote oscillations in cytoplasmic free Ca^{2+} concentration in the pancreatic β-cell. *Proc. Natl. Acad. Sci. USA.* 93:5161–5165.

Ma, M., and J. Koester. 1996. The role of K^+ currents in frequency-dependent spike broadening in *Aplysia* R20 neurons: a dynamic-clamp analysis. *J. Neurosci.* 16:4089–4101.

Meissner, H. P., and W. Schmeer. 1981. The significance of calcium ions for the glucose-induced electrical activity of pancreatic β-cells. *In* The Mechanism of Gated Calcium Transport across Biological Membranes. S. T. Ohnishi and M. Endo. Academic Press, New York. 157–165.

Misler, S., D. W. Barnett, K. D. Gillis, D. M. Pressel. 1992. Electrophysiology of stimulus-secretion coupling in human beta-cells. *Diabetes.* 41:1221–1228.

Misler, S., L. C. Falke, K. Gillis, and M. L. McDaniel. 1986. A metabolite-regulated potassium channel in rat pancreatic B cells. *Proc. Natl. Acad. Sci. USA.* 83:7119–7123.

Misler, S., D. M. Pressel, and K. D. Gillis. 1991. Depolarization-secretion coupling in pancreatic islet B cells: do diverse excitability patterns support insulin release? *In* Proceedings of the 14th Congress of the International Diabetes Federation. Elsevier Publishers, Amsterdam, The Netherlands.

Miura, Y., J. C. Henquin, and P. Gilon. 1997. Emptying of intracellular Ca^{2+} stores stimulates Ca^{2+} entry in mouse pancreatic beta-cells by both direct and indirect mechanisms. *J. Physiol. (Lond.).* 503:387–398.

O'Neil, M. B., L. F. Abbott, A. A. Sharp, and E. Marder. 1995. Dynamic clamp: computer-neural hybrids. *In* Handbook of Brain Theory and Neural Networks. M. Arbib, editor. 326–329.

Ribalet, B., and P. M. Beigelman. 1980. Calcium action potential and potassium permeability activation in pancreatic β-cells. *Am. J. Physiol.* 239:C124–C133.

Ribalet, B., and P. M. Beigelman. 1981. Effects of divalent cations on beta-cell electrical activity. *Am. J. Physiol.* 241:C59–C67.

Rorsman, P., and G. Trube. 1985. Glucose dependent K^+-channels in pancreatic β-cells are regulated by intracellular ATP. *Pflügers Arch.* 405:305–309.

Rorsman, P., and G. Trube. 1986. Calcium and delayed potassium currents in mouse pancreatic β-cells under voltage-clamp conditions. *J. Physiol. (Lond.).* 374:531–550.

Rosario, L. M., I. Atwater, and A. M. Scott. 1986. Pulsatile insulin release and electrical activity from single ob/ob mouse islets of Langerhans. *Adv. Exp. Med. Biol.* 211:413–425.

Santerre, R. F., R. A. Cook, R. M. Crisler, J. D. Sharp, R. J. Schmidt, D. C. Williams, and C. P. Wilson. 1981. Insulin synthesis in a clonal cell line of simian virus 40-transformed hamster pancreatic beta cells. *Proc. Natl. Acad. Sci. USA.* 78:4339–4343.

Satin, L. S. 1996. New mechanisms for sulfonylurea control of insulin secretion. *Endocrine.* 4:191–198.

Satin, L. S., and D. L. Cook. 1988. Evidence for two calcium currents in insulin-secreting cells. *Pflügers Arch.* 411:401–409.

Satin, L. S., and D. L. Cook. 1989. Calcium inactivation in insulin secreting cells is mediated by calcium influx and membrane depolarization. *Pflügers Arch.* 414:1–10.

Satin, L. S., T. A. Kinard, A. Sherman, and G. de Vries. 1996. Dynamic clamping of excitable cells: a window into the role of ion channels in cell excitability. *Axobits.* 19:8–9.

Satin, L. S., and P. D. Smolen. 1994. Electrical bursting in β-cells of the pancreatic islets of Langerhans. *Endocrine.* 2:677–687.

Satin, L. S., S. J. Tavalin, T. A. Kinard, and J. Teague. 1995. Contribution of L- and non-L-type calcium channels to voltage-gated calcium current and glucose-dependent insulin secretion in HIT-T15 cells. *Endocrinology.* 136:4589–4601.

Satin, L. S., S. J. Tavalin, and P. D. Smolen. 1994. Inactivation of HIT Ca^{2+} current by a simulated burst of Ca^{2+} action potentials. *Biophys. J.* 66:141–148.

Sharp, A. A., M. B. O'Neil, L. F. Abbott, and E. Marder. 1993. Dynamic clamp: computer-generated conductances in real neurons. *J. Neurophysiol.* 69:992–995.

Sherman, A. 1996. Contributions of modeling to understanding stimulus-secretion coupling in pancreatic β-cells. *Am. J. Physiol.* 34:E362–E372.

Sherman, A., J. Rinzel, and J. Keizer. 1988. Emergence of organized bursting in clusters of pancreatic β-cells by channel sharing. *Biophys. J.* 54:411–425.

Smith, P. A., F. M. Ashcroft, and P. Rorsman. 1990. Simultaneous recording of glucose dependent electrical activity and ATP-regulated K^+-currents in isolated mouse pancreatic β-cells. *FEBS Lett.* 261:187–190.

Smolen, P. D., J. Rinzel, and A. Sherman. 1993. Why pancreatic islets burst but single β cells do not: the heterogeneity hypothesis. *Biophys. J.* 64:1668–1680.

Sturgess, N. C., M. L. J. Ashford, D. L. Cook, and C. N. Hales. 1985. Sulfonylurea receptor may be an ATP-sensitive potassium channel. *Lancet.* 2:474–475.

Trube, G., P. Rorsman, and T. Ohno-Shosaku. 1986. Opposite effects of tolbutamide and diazoxide on the ATP-dependent K^+ channel in mouse pancreatic β-cells. *Pflügers Arch.* 407:493–499.

Turrigiano, G. G., E. Marder, and L. F. Abbott. 1996. Cellular short-term memory from a slow potassium conductance. *J. Neurophysiol.* 75: 963–966.